

CDKL5 Regulates Flagellar Length and Localizes to the Base of the Flagella in *Chlamydomonas*

Lai-Wa Tam, Paul T. Ranum and Paul A. Lefebvre

Department of Plant Biology, University of Minnesota, St. Paul, MN 55108

Address correspondence to Paul A. Lefebvre, Department of Plant Biology, University of Minnesota, 250 BioScience Center, 1445 Gortner Ave., St. Paul, MN 55108

Tel: (612) 624-0729 Fax: (612) 625-1738 Email: pete@umn.edu

Running title: CDKL5 Regulates Flagellar Length

Abbreviations: CDK, cyclin-dependent kinase; CDKL, cyclin-dependent kinase-like; DIC, differential interference microscopy; IFT, intraflagellar transport; LF, long flagella; LRC, length regulatory complex; MAPK, mitogen-activated protein kinase; WT, wild type.

Abstract

The length of *Chlamydomonas* flagella is tightly regulated. Mutations in four genes, *LF1*, *LF2*, *LF3* and *LF4*, cause cells to assemble flagella up to three times wild-type length. *LF2* and *LF4* encode protein kinases. Here we describe a new gene, *LF5*, in which null mutations cause cells to assemble flagella of excess length. The *LF5* gene encodes a protein kinase very similar in sequence to the protein kinase CDKL5. In humans, mutations in this kinase cause a severe form of juvenile epilepsy. The LF5 protein localizes to a unique location—the proximal 1 μm of the flagella. The proximal localization of the LF5 protein is lost when genes that make up the proteins in the cytoplasmic length regulatory complex (LRC), *LF1*, *LF2* and *LF3*, are mutated. In these mutants LF5p becomes localized either at the distal tip of the flagella or along the flagellar length, indicating that length regulation involves, at least in part, control of LF5p localization by the LRC.

Introduction

Interest in the control of the assembly of cilia and flagella has greatly increased in recent years with the discovery that many human diseases are caused by defects in cilia (Badano *et al.*, 2006; Berbari *et al.*, 2009). A particularly intriguing aspect of flagellar assembly is the highly regulated control of flagellar length in the unicellular green alga, *Chlamydomonas* (reviewed by Wemmer and Marshall, 2007; Wilson *et al.*, 2008). The genetic regulation of flagellar length in *Chlamydomonas* has been uncovered by analyzing the phenotypes and underlying molecular lesions of mutants in which the flagella assemble to lengths either longer or shorter than the flagella of wild-type (WT) cells (Kuchka and Jarvik, 1987; Barsel *et al.*, 1988; Asleson and Lefebvre, 1998). Mutants that cause flagella to assemble to excessive length, up to 2 to 3 times the 14 μm length of flagella of WT cells, have been shown to identify four unlinked genes that control the extent of flagellar assembly. Two of these genes, *LF2* and *LF4* encode kinases of the cyclin-dependent kinase (CDK) family (Tam *et al.*, 2007) and the mitogen-activated protein kinase (MAPK) family, respectively (Berman *et al.*, 2003).

Three of the four long-flagella (*LF*) genes encode proteins that interact with each other and are found exclusively in the cytoplasm and not the flagella. The proteins, LF1p, LF2p and LF3p, are found together in complexes called Length Regulatory Complexes (LRC) (Tam *et al.*, 2003; 2007; Nguyen *et al.*, 2005). These three proteins have been shown to interact by a variety of methods, including co-fractionation and pair-wise yeast two-hybrid experiments. All three proteins localize to punctate structures in the cytoplasm using immunofluorescence microscopy. In addition, any double mutant combination of *lf1*, *lf2* and *lf3* alleles produces cells with severe flagellar assembly defects (Barsel *et al.*, 1988; Asleson and Lefebvre, 1998). Double mutant cells assemble either a single flagellum or no flagella.

The fourth *LF* gene, *LF4*, encodes a MAPK localized in both the flagella and the cytoplasm (Berman *et al.*, 2003). *lf4* mutants have been isolated repeatedly as insertional mutants, presumably because the long-flagella phenotype is the null mutant phenotype. By contrast, null mutants in *lf2* and *lf3* have been shown to have a more severe flagellar phenotype known as “UIF” for “unequal length flagella” (Tam *et al.*, 2003; 2007). These mutants are either flagella-less, or if they have flagella they often have two flagella of unequal length, each shorter than WT flagella.

We have recently isolated two new insertional mutant alleles that identify a fifth *LF* locus, *LF5*. *lf5* mutants have long flagella, but not as long as *lf4*. *LF5* encodes a protein kinase with a high degree of sequence homology in the kinase domain to human cyclin-dependent kinase-like (CDKL) kinase, CDKL5. A remarkable feature of LF5p is that it localizes to the proximal 1 μ m of the flagella, a localization observed for very few flagellar proteins. This kinase is of particular interest in humans, as a number of different lesions in CDKL5 lead to severe juvenile epilepsy of unknown etiology (Kalscheuer *et al.*, 2003; Rademacher *et al.*, 2011; Kilstup-Nielsen *et al.*, 2012). The identification of *LF5* in *Chlamydomonas* as a gene controlling flagellar length raises the possibility that ciliary length plays an important role in early brain development, and that defects in ciliary length control may be involved in the development of juvenile epilepsy.

Results

Phenotype of two new *LF* mutants

Exogenous DNA, when transformed into *Chlamydomonas*, can randomly integrate into the nuclear genome and cause mutations in different genes. Previously, all of the mutants with long flagella (*LF*) phenotype created by this method were alleles of a single gene, *LF4* (Asleson and Lefebvre, 1998). We recently identified two insertional *LF* mutants, 3F12 and DKD6, that identify a previously unknown *LF* locus, *LF5*. When crossed to each other, 3F12 and DKD6 gave rise to progeny that only have the long-flagella phenotype (14 tetrads), indicating that these two mutants are either allelic or very closely linked.

In contrast to *lf4* mutants, which have very long flagella at least twice the length of flagella of WT cells, 3F12 and DKD6 have moderately long flagella, with average lengths that are 1.3-1.5 times the length of flagella of WT cells (Figure 1A). All mutant cells move erratically and slowly. Among the previously identified *lf* mutants, *lf4* mutants have flagella with tapered ends similar to those seen on the flagella of WT cells, while certain mutant alleles in *lf1*, *lf2* or *lf3* have flagella with distal tips that appear to be swollen. The swollen flagellar tips in these mutants are accompanied by an accumulation of intraflagellar transport proteins at the tips (Tam *et al.*, 2003). Mutants 3F12 and DKD6, however, have flagella that are more similar in morphology to those of *lf4* mutants, having no distal swelling (Figure 1B).

Many *lf1*, *lf2* and *lf3* mutant alleles show severe impairment in their ability to regrow flagella after amputation (Barsel *et al.*, 1988). To test whether DKD6 cells can regenerate their flagella, the length of the flagella were measured at different times after pH-induced deflagellation. In three separate experiments, we found that DKD6 cells were able to regrow their flagella, though less synchronously and more slowly than WT cells. A representative experiment is illustrated in Figure 1C, showing the lower average lengths and wider range of flagellar lengths of DKD6 compared to those of WT at time points between 15-60 min after pH shock.

Mapping and cloning of *LF5*

Unfortunately, the mutant lesions in the DKD6 and 3F12 strains were not caused by the insertion of the plasmids used in transformation, so map-based cloning was used to obtain the *LF5* gene. To map the mutation in 3F12, we performed a cross of 3F12 with the polymorphic *C. reinhardtii* strain S1 D2, and performed PCR to check the linkage of the *lf* mutation with molecular markers on each chromosome. This mapping placed the *lf* mutation on chromosome 12, linked to the markers *TUB2* and *RDB* (Table 1). Based on the genomic sequences of the polymorphic *C. reinhardtii* strains, we designed additional mapping primers on chromosome 12 around the region of interest to further delineate the location of the mutation. The closest markers that recombined with this *lf* mutation are 14-3-3 at 4.3 cM on one side and 5750 at 3.3 cM on the other side (Table 1). All other markers, defining a physical distance of about 1000 kb between these two markers, including the centromere, did not recombine with the mutation, probably due to suppression of recombination around the centromere. The mapped location of this new *LF* mutation is distinct from *LF2*, which is also on chromosome 12 but at the distal portion of one arm. Therefore, 3F12 defines a new *LF* locus, designated as *LF5*.

Having obtained detailed mapping information for *LF5*, we next used a candidate gene approach to clone the gene. Because analysis of the four known *LF* genes strongly suggests the involvement of protein kinases in flagellar length control, we designed primers to test for genetic lesions in protein kinases among the candidate gene models. An insertion in the gene model FAP247, a protein kinase previously found in the flagellar proteome (Pazour *et al.*, 2005) was detected in 3F12 (Figure 2, A and B). Chlamydomonas DNA fragments covering this gene model cloned in lambda phage ($\lambda 5$, $\lambda 6$, $\lambda 12$) or in pBluescript (pBS3830) were transformed into the mutant. Only clones containing the entire FAP247 gene were able to rescue 3F12 to the WT phenotype (Figure 2A). To determine the location of the insertion in 3F12, a bacteriophage lambda library was made using DNA from 3F12 and clones containing the mutant gene were obtained and characterized. A piece of Chlamydomonas DNA from an unmapped scaffold was found in intron 8 of FAP247. Presumably, during the transformation experiment that produced this mutant, a fragment of unrelated DNA from the Chlamydomonas genome was inserted into the *LF5* gene.

Restriction fragments of FAP247 identified by the same hybridization probe were also polymorphic in the second mutant, DKD6 (Figure 2B). Further analysis revealed that the 1.8 kb *SacI* fragment at the upstream region of FAP247 (Figure 2A) was missing in DKD6 (data not shown). DKD6 was rescued with pBS3830, showing that DKD6 contains an *lf5* mutant allele. The two alleles are designated as *lf5-1* in 3F12 and *lf5-2* in DKD6.

LF5p is a CDKL kinase

To determine the coding sequence of *LF5*, six clones spanning 2440 bps were recovered from a cDNA library. The cDNA sequence (GenBank accession number: KC297221) contains a large open reading frame that is predicted to encode a protein, *LF5p*, of 622 amino acids with a

calculated mass of 66,643. The N-terminal 291 residues of LF5p contain the 11 kinase subdomains characteristic of serine/threonine protein kinases (Figure 3A). BLAST searches reveal that LF5p is a member of the cyclin-dependent kinase-like (CDKL) kinase subfamily. There are five different CDKL kinases in humans, which are distant relatives of CDK kinases that also share common characteristics with MAPK kinases. CDKLs, for example, have a TE/DY motif, characteristic of MAPK, in the activation loop. Interestingly, two other genes in which mutations produce a long-flagella phenotype, *LF2* and *LF4*, encode a CDK-related kinase and a MAPK, respectively. Figure 3B shows the phylogenetic relationship of these three *Chlamydomonas* kinases with their closest human orthologs and the five human CDKL kinases. LF5p is most homologous to CDKL5 (Figure 3C; 80% similar/ 62% identical and 81% similar/65% identical to human and *Tetrahymena* CDKL5, respectively). The human CDKL5 protein exists in multiple isoforms with different C-terminal regions produced by alternative splicing (Williamson *et al.*, 2012). The longest isoform has a C-terminal tail of 750 residues. LF5p has a C-terminal domain of 331 residues (Figure 3A). This C-terminal domain does not share significant homology to other CDKL5 proteins, nor does it contain any obvious sequence motifs. Analysis of LF5p using NetPhos 2.0 (<http://www.cbs.dtu.dk/services/NetPhos/>) identified 22 very likely sites of (scores > 0.9) S/T/Y phosphorylation, of which 15 are in the C-terminal tail. Given the well-established roles of other kinases in regulating flagellar length, phosphorylation of LF5p may play important roles in *LF5* function.

***LF5* is up-regulated by deflagellation and encodes a flagellar protein**

To identify the RNA transcript of *LF5*, total RNAs from WT and *lf5* mutants were fractionated on RNA blots and hybridized with a probe made from the entire coding region of *LF5*. In WT cells, a 4-kb transcript was detected (Figure 2C). This transcript was not detectable in either *lf5-1* (3F12) or *lf5-2* (DKD6); however, a small transcript of 1.5 kb hybridized to the *LF5* probe when RNA from *lf5-1* was examined (Figure 2C). Based on the location of the inserted DNA in *lf5-1* and the size of this aberrant transcript, it appears that the insertion caused an early termination of transcription, producing a chimeric transcript containing only the first eight exons of *LF5* (1 kb) and part of the inserted DNA. On the contrary, *lf5-2*, which appeared to have a deletion within the genomic region, was likely to be a null mutant not producing any stable RNA product. We detect no differences in flagellar length or function between the two *lf5* mutant alleles, suggesting that they are both effectively null alleles of the *LF5* locus.

Previous genome-wide transcriptional analysis and real time RT-PCR indicated that FAP247 (*LF5*) RNA transcript was induced upon deflagellation (Pazour *et al.*, 2005; Stolc *et al.*, 2005). We examined poly(A)⁺ RNA isolated from WT cells at different times after deflagellation to characterize in more detail the expression of *LF5* transcript. We found that the level of *LF5* transcript increased rapidly to >4-fold 15 min after deflagellation and reached a maximum level of > 5-fold at 30 min (Figure 2D). This result shows that the increase of *LF5* RNA accumulation occurs quickly as cells start to regenerate their flagella.

LF5p can be dissociated from axonemes with high salt

An affinity-purified antibody prepared using recombinant histidine-tagged LF5p as immunogen specifically recognized a major protein product that migrated at ~66 kDa and a minor product at ~45 kDa in WT flagella, but not in *lf5* mutant flagella (Figure 4A, left panel). The size of the major band is in agreement with the predicted size of LF5p from sequence analysis. The minor band may be a truncated or degraded fragment of LF5p. Some smaller proteins were also detected but all of them were equally abundant in WT and both *lf5* mutant flagella, indicating they represent non-specific interaction with the antibody. The 66-kDa and

45-kDa protein bands were also detected in the flagella of *lf1* or *lf4* mutants, suggesting that mutations in other *LF* genes do not affect the accumulation of LF5p in flagella.

To assess which flagellar compartment(s) contain LF5p, WT flagella were extracted with 0.5% NP40 to obtain the soluble matrix/membrane fraction. Only a small fraction of LF5p was present in the NP-40 soluble fraction, with the majority of LF5p remaining in the demembrated axonemes (Figure 4A, right panels). The majority of LF5p could be solubilized from demembrated axonemes by treatment with 0.5 M NaCl or 0.6 M KI (Figure 4A), consistent with the earlier finding that the five unique tryptic peptides of FAP247 were identified mostly from KCl extracts of axonemes (Pazour *et al.*, 2005). The extractability of LF5p by 0.5 M NaCl indicates that ionic interactions are critical to axonemal binding of LF5p.

LF5p is localized to the very proximal region of flagella

We used the LF5 antibody to localize LF5p in flagella by indirect immunofluorescence, using an acetylated α -tubulin antibody for co-localization to identify the location of flagella, basal bodies and microtubule rootlets. In WT cells, bright staining was observed in the very proximal region ($\sim 0.5 \mu\text{m}$) of the flagella, (Figure 4B, a-c). A small amount of punctate staining was also observed on some of the flagella. Such flagellar staining was not observed in *lf5-1* and *lf5-2* cells, showing the specificity of the flagellar fluorescence signal (Figure 4B, d-f). Cytoplasmic spots of staining were observed with the antibody in some experiments. However, these spots appeared to be present similarly in both WT and *lf5* mutant cell bodies, indicating that they do not represent LF5p localization in the cell cytoplasm.

In each *Chlamydomonas* cell there are two mature basal bodies that nucleate the formation of two flagella. When cells shed their flagella, the flagella break distal to a structure at the end of the body known as the transition zone (Craigie *et al.*, 2010), so that the transition zone remains with the basal bodies in the cell (Sanders and Salisbury, 1989). Three observations indicate that the LF5p is localized to the flagella but not the transition zones or the basal bodies. First, bright proximal staining was observed on flagella that had been detached from the cells during the fixation process (Figure 4B, g-i). Second, when flagella were amputated by pH shock, all staining in the cell near the basal body region was lost (Figure 4B, j-l). Third, in the *uni2-3* mutant, which often forms a single flagellum from one of the two basal bodies, only one bright spot was seen in the proximal region of the flagellum (Figure 4B, m-o) in cells that had only a single flagellum.

Rapid sequestration of LF5p to the proximal region of growing flagella

To determine how rapidly LF5p becomes proximally localized during flagellar assembly, we examined cells undergoing flagellar regrowth after deflagellation (Figure 5). At 15 min after pH shock, when the regenerating flagella were $3.4 \mu\text{m}$ long on average ($\sim 30\%$ of pre-deflagellated length), we could detect proximal staining. However, 100% of the flagella also showed punctate staining along the flagella during this stage, probably reflecting the ongoing deposition of LF5p into the flagellum (Figure 5, A-C). As the flagella continued to grow, the proximal stain became brighter (Figure 5, D-F) and the percentage of flagella with punctate staining along the length in addition to proximal staining decreased to 82.1%, 45.4% and 14.8% at 30 min, 60 min and 120 min, respectively.

Disassembly of flagella can also be induced by calcium chelators such as 20 mM sodium pyrophosphate (Lefebvre *et al.*, 1978). Cells treated with pyrophosphate shorten their flagella, with approximately 50% of the flagellar length resorbed into the cell within 60 min of treatment. We examined the localization of LF5p in cells treated with pyrophosphate during a 2-hour period in which the cells gradually resorbed their flagella. The proximal staining of LF5p remained

prominent throughout resorption, independent of the length of the flagella (Figure 5, G-L). Unlike growing flagella, LF5p staining was infrequently observed along the length of resorbing flagella.

Proximal LF5p localization is not affected by many flagellar mutations

To determine whether LF5p may be associated with any of the known axonemal structures, LF5p was localized using indirect immunofluorescence in mutants missing or defective in radial spokes (*pf14*, *pf27*; Luck *et al.*, 1977; Huang *et al.*, 1981; Diener *et al.*, 1993), the central pair (*pf15*, *pf16*, *pf19*, *pf20*; Witman *et al.*, 1978; Dutcher *et al.*, 1984; Smith and Lefebvre, 1996; 1997; Dymek and Smith, 2012), inner dynein arms (*pf9*, *pf23*, *ida5*; Piperno *et al.*, 1990; Mastronarde *et al.*, 1992; Kato-Minoura *et al.*, 1997; King and Dutcher, 1997; Myster *et al.*, 1997) and outer dynein arms (*pf28*; Kamiya, 1988), as well as the dynein regulatory complex (*pf3*; Piperno *et al.*, 1992; Gardner *et al.*, 1994). Bright proximal staining of LF5p was observed in all these cases, suggesting LF5p is not part of these structures (representative examples for each type of axonemal mutants are shown in Figure 6A). Proximal localization of LF5p also was observed in *mbo2*, which lacks doublet microtubule-specific beak projections residing in the proximal one-third of flagella (Segal *et al.*, 1984). These results suggest that LF5p does not associate with axonemal structures we analyzed here, which all occur with regular periodicity along the axonemes. It is possible that LF5p associates directly with the doublet microtubules of the axoneme.

Two Chlamydomonas proteins have been localized to the proximal regions of flagella. DHC11, an inner-arm heavy chain dynein, was localized to the proximal 2 μ m of flagella (Yagi *et al.*, 2009). In the *ida5* mutant, which does not assemble DHC11 in its flagella, localization of LF5p to the proximal ends of flagella was indistinguishable from the localization seen in WT flagella (Figure 6B, a-c). *FA2*, which encodes a NIMA kinase important for calcium-dependent deflagellation, localizes tightly to the proximal end of the flagella, as well as around the basal bodies (Mahjoub *et al.*, 2004). We examined both *fa1* and *fa2* mutants, which are defective in the same pathway, but did not detect any change in LF5p localization (Figure 6B, d-f). At least two proximally-localized axonemal proteins, therefore, play no role in proximal localization of LF5p.

Flagellar assembly and disassembly in Chlamydomonas requires intraflagellar transport (IFT), and in mutants with defects in IFT the localization of flagellar proteins can be altered (e.g. Pazour *et al.*, 1998; Pedersen *et al.*, 2005). We examined localization of LF5p on the flagella of two IFT mutants with defective IFT. The *fla11* mutant has a genetic lesion in IFT172, and is thought to have defects in the remodeling of IFT particles at the flagellar tip to prepare for the change from anterograde to retrograde transport (Pedersen *et al.*, 2005). The *fla14* mutant is defective in the dynein light chain LC8, and as a result of defects in the cytoplasmic dynein complex *fla14* lacks retrograde IFT (Pazour *et al.*, 1998). Indirect immunofluorescence localization showed proximal localization of LF5p in both mutants, indistinguishable from the localization in the flagella of WT cells (Figure 6B, g-l). While IFT may be involved in the transport of LF5p to the flagella, this result suggests that IFT, particularly retrograde IFT, probably has no direct regulatory role in the proximal localization of LF5p in flagella.

LF5p proximal localization is affected by mutations in *LF1*, *LF2* and *LF3*

Previous studies showed that LF1p, LF2p and LF3p reside in a protein complex, the LRC, in the cell body (Tam *et al.*, 2007), while LF4p is present both in the cell body and the flagella (Berman *et al.*, 2003). To assess the effect of mutations of these four *LF* genes on the localization of LF5p, immunofluorescence studies with the LF5 antibody were performed on

various *lf* mutant alleles, including *lf1-1*, *lf2-1*, *lf2-3*, *lf2-5*, *lf3-2* and *lf4-9*. Strikingly, the proximal localization of LF5p was greatly diminished or absent in various mutant alleles of *LF1*, *LF2* and *LF3*. Instead, in these mutants, bright staining of LF5p was often observed at the distal tips of flagella (representative examples are shown in Figure 7, A-P). Proximal and distal staining were not mutually exclusive - both could be seen on the same flagellum (Figure 7, E-H). In addition, punctate staining was observed along some flagella (Figure 7, M-P). In contrast, LF5p remained localized predominantly to the proximal ends of flagella in *lf4-9*, though punctate staining also appeared to be present along the length (Figure 7, Q-T). We quantified the percentage of flagella showing different LF5p localization: proximal, distal, both proximal and distal or only along the entire length of flagella (Table 2). Though the localization patterns were variable among different LRC mutants, all of them showed a striking shift of LF5p staining from proximal to distal ends of flagella. These results raise the interesting possibility that LF5p is a target of the LRC, perhaps regulating flagellar length, at least in part, by regulating the localization of LF5p in flagella.

The possibility that the proximal localization of LF5p is critically important for its function in length control is supported by experiments to localize the protein during mating. When *Chlamydomonas* cells mate, the flagella adhere to each other, leading within about 10 min to cell fusion to form a single cell with four flagella and two nuclei, known as a dikaryon. When *lf* mutants are mated to WT cells, the long flagella are resorbed to WT length by 90 min, indicating that flagellar length control is a dynamic and regulated process, and that the *lf* mutations are recessive (Barsel *et al.*, 1988). We localized LF5p in flagella before and at different time points after mating *lf1* mutants to WT cells. In flagella of *lf1* gametes before mating, most labeling using the LF5 antibody was not at the proximal region, but at the distal tip or along the length of the flagella (92% of cells). At 15 minutes after mating, 32% of mating dikaryons still showed two flagella with proximal labeling (the WT flagella) and two flagella with label along the length or at the distal tip (the *lf1* flagella; Figure 8A, a-c). However proximal labeling was clearly observable on all four flagella in 40% of dikaryons (Figure 8A, g-i). In addition, 28% of dikaryons also showed partial re-localization of LF5p to one of the two long flagella that originate from the *lf1* parent (Figure 8A, d-f). The percentage of dikaryons showing four proximal spots increased to 60% and 73% at 30 min and 45 min respectively. Importantly, the movement of LF5p to the proximal end of the long flagella preceded the complete resorption of the flagella to WT length. While striking re-localization of LF5p was observed as early as 15 min after mating, the length of the longer pair of flagella in these dikaryons was largely indistinguishable from the length of the flagella of the *lf1* parent (Figure 8B). The kinetics of movement of the LF5 protein to the proximal end before flagellar resorption indicates that the proximal labeling is not a consequence of restoration of length control and may, in fact, be causal for resorption.

Discussion

What does the proximal localization of LF5p tell us about flagellar length control?

LF5p is unique among the proteins known to be involved in flagellar length control in its localization to the very proximal end of the flagella. Interestingly, the function of the other *LF* gene products identified as components of the LRC may be involved in LF5p localization. Proximal localization of LF5p is either reduced or eliminated by the defects in *lf1*, *lf2*, or *lf3* mutants. The fact that *lf1*, *lf2* and *lf3* mutants cause LF5p to be mis-localized along the length and even at the distal end of flagella, suggests that one role of the LRC may be to restrict LF5p

to the proximal end of the axoneme. It is unlikely that the sole role for the LRC proteins is to control LF5p localization, however, because *lf1*, *lf2* and *lf3* mutants are all significantly longer than *lf5* mutants (Barsel *et al.*, 1988). One possible role for a proximally-located kinase might be to regulate entry of proteins into the flagella, including length control proteins such as LF4p. A kinase at the proximal end of the flagella could also be part of a length-sensing mechanism. If, for example, phosphorylation of some unidentified sensor protein occurs as it enters the flagella, and de-phosphorylation of such a protein by phosphatases occurs at a constant rate as it is transported to the distal end, then the phosphorylation state of this protein could be used to inform an assembly-regulating mechanism at the tip of the length of the flagella. A potential candidate protein whose phosphorylation state is regulated by flagellar length has been identified (Luo *et al.*, 2011). The *Chlamydomonas* flagellar aurora-like kinase CALK exists in either a phosphorylated and a non-phosphorylated form, and the phosphorylation state appears to be directly related to flagellar length. When flagella are 6 μm or less in length, CALK is phosphorylated, but longer flagella contain only non-phosphorylated CALK. If phosphorylated CALK is itself involved in regulating a protein essential for flagellar growth, presumably by phosphorylation, then CALK and LF5p, along with LF4p may work together to tightly regulate flagellar length.

Although the placement of LF5p at the proximal end of the flagella suggests that regulation of flagellar length occurs at that end, there are a number of reasons to predict regulation at the distal tip as well. Assembly of both tubulins, the major structural protein of the axoneme (Witman, 1975) as well as other flagellar proteins (Johnson and Rosenbaum, 1992) occurs at the tip. Anterograde IFT has been shown to be required for transport of flagellar proteins to the flagellar tip for assembly (reviewed by Scholey, 2003; Qin *et al.*, 2004). Proteins at the flagellar tip have been implicated in re-modeling the IFT protein machinery for the transition from anterograde to retrograde transport (Pedersen *et al.*, 2005), and this remodeling and its implications for control of assembly has been used as the basis for a model for control of flagellar length (Engel *et al.*, 2009). The movement of LF5p from the proximal to the distal end of the flagella in *lf1*, *lf2* and *lf3* mutants may play a role in the assembly of flagella of excessive length, or it could be a consequence of loss of flagellar length control. Movement of LF5p to the distal end is not a requirement for assembling aberrantly long flagella, however, because LF5p remains at the proximal end of long flagella in *lf4* mutants.

We do not yet know how LF5p localization is restricted to the proximal end of the flagella of WT cells. The protein could be actively transported (from the tip?) to the proximal end and retained there by binding to a proximally-localized binding target, or it could simply bind to the proximal end soon after the protein enters the flagella. The former possibility is consistent with the observation (Figure 5) that during flagellar regeneration LF5p is initially localized along the length of the flagella and then later becomes exclusively localized to the proximal end. Also supporting this active movement is the observation that when mutants with long flagella, in which LF5p is localized at the distal tip or along the flagellar length, are mated to WT cells, LF5p rapidly moves to the proximal end of the flagella, even before the long flagella are restored to WT length (Figure 8A). Surprisingly, however, retrograde IFT is not an absolute requirement for localization of LF5p to the proximal end of the flagella because in the flagella of *fla11* and *fla14*, which have defective retrograde IFT, LF5p is still localized to the proximal end.

A unique feature of *LF5* relative to the other length-control genes is that flagellar length appears to still be regulated in *lf5* mutants, but to a longer length than WT. Whereas mutants in

lf1, *lf2*, *lf3* and *lf4* have a broad distribution of flagellar lengths, from shorter than WT to 2 to 3 times WT, a population of *lf5* cells has a tighter distribution of flagellar lengths centered around a point approximately 50% longer than the flagella length of WT cells (Figure 1). From the length distribution curves it appears that mutants in the other *LF* genes lose flagellar length control, but that *lf5* mutants retain length control, though the target length is increased relative to WT. The intriguing possibility raised by this observation is that *LF5* may be involved in setting the appropriate flagellar length, as opposed to enforcing length control.

The majority of LF5p is tightly associated with doublet microtubules in an NP-40 insoluble fraction. Given that we cannot find evidence for association of the protein with any known axonemal structures, such as dynein arms or radial spokes, the interesting possibility exists that LF5p binds directly to the doublet microtubules of the axoneme, localizing to only the proximal 1 μ m by an as yet unknown mechanism. Clearly the proteins of the LRC in some way help localize LF5p to the proximal end of the axoneme, as *lf1*, *lf2* and *lf3* mutations cause LF5p to localize along the length of the axoneme and at the distal tip. Perhaps these proteins modify LF5p, most likely through the kinase activity of LF2p, to make it bind to its proximal location. Alternatively, they could modify the proximal end of the axoneme to provide a binding site for LF5p.

The role of protein kinases in flagellar length control

The characterization of a new protein kinase associated with flagellar length control adds to a growing realization that this control is a highly regulated and complex process involving numerous cell-signaling inputs. Not only have three kinases (LF2p, LF4p, and LF5p) been shown directly by mutation to be involved in length control, experiments point to the role of several other kinases in sensing and controlling flagellar length. For example, lithium ions cause *Chlamydomonas* flagella to grow up to 30% longer than untreated flagella, possibly by inhibiting another flagellar kinase, glycogen synthase kinase 3 (GSK3; Wilson and Lefebvre, 2004). Recently a set of experiments analyzing inhibitor effects on GSK3 and other kinases showed that in mammalian cells lithium ions cause increases in the length of primary cilia through effects on cAMP-activated protein kinases (Ou *et al.*, 2009). Another protein kinase in *Chlamydomonas*, the NIMA-related kinase, CRK2p, was implicated in flagellar length control by experiments in which levels of the kinase were reduced by RNA interference. Reduced levels of CRK2p resulted in increased flagellar length, up to 40%, accompanied by increased cell volume (Bradley and Quarmby, 2005).

Possible role of CDKL5 in juvenile epilepsy

A role for CDKL5 in human brain development is suggested by the association of epileptic seizures in early childhood with defects in this protein. It is not known how defects in CDKL5 lead to juvenile epilepsy. CDKL5 in human cells localizes both to the nucleus and the cytoplasm (Rusconi *et al.*, 2008), with nuclear localization being associated with speckles and therefore perhaps with the splicing machinery (Ricciardi *et al.*, 2009). Human CDKL5 has been shown to interact with a number of other proteins, including DNA methyltransferase I protein (Dnmt1), which in turn has been shown to interact with the methyl-cytosine binding protein MeCP2 (Kameshita *et al.*, 2008). MeCP2 is the gene affected in the majority of cases of Rett syndrome, a form of juvenile epilepsy with similar features to CDKL5 disease (reviewed by Grillo *et al.*, 2012). Another protein interacting with CDKL5 is Rac1, an important protein in actin remodeling and neuronal patterning (Chen *et al.*, 2010). Inhibition of Rac1 in tissue culture cells has been shown to alter the localization of the basal bodies that subtend the cilia (Hashimoto *et al.*, 2010), suggesting a possible link between human CDKL5 and cilia.

Although there is as yet no evidence that CDKL5 is a ciliary protein in any system besides *Chlamydomonas*, a ciliary localization could help explain the unexplained role of CDKL5 mutations in causing juvenile epilepsy. A suggestion that a different form of epilepsy, juvenile myoclonic epilepsy, might be associated with defects in the ciliary axoneme also came from studies in *Chlamydomonas*. Genetic studies indicated that juvenile myoclonic epilepsy is associated with the EFHC1 gene, which structural analysis suggested was a close structural homologue of the *Chlamydomonas* Rib72 gene, which encodes a protein required for the assembly of the flagellar axoneme (King, 2006). The possibility that CDKL5 could be a ciliary protein in humans would add another set of diseases, juvenile epilepsies, to the growing list of diseases whose etiology appears to be associated with defective cilia and flagella, diseases that have been termed “ciliopathies” (Badano *et al.*, 2006; Berbari *et al.*, 2009).

Materials and Methods

Strains, culture conditions and genetic analysis

Strains obtained from the *Chlamydomonas* Resource Center (University of Minnesota) are: CC-1690 (21 gr), CC-125 and CC-621 (WT), CC-1952 (polymorphic strain S1 D2), CC-1678 (*lf1-1*), CC-803 (*lf2-1*), CC-2287 (*lf2-5*), CC-2289 (*lf3-2*), CC-1026 (*pf3*), CC-1032 (*pf14*), CC-1033 (*pf15*), CC-1038 (*pf20*), CC-1877 (*pf28*), CC-1383 (*pf23*), CC-3421 (*ida5*), CC-3898 (*pf9*), CC-1370 (*fa1*), CC-3751 (*fa2*), CC-1920 (*fla11*), CC-3937 (*fla14*), CC-2377 (*mbo2*), CC-4162 (*uni2-3*). Cells were grown in liquid M or TAP medium under continuous light. 3F12 and D12 (*lf4-9*) were obtained by DNA insertion into the genome of strain of 21 gr. DKD6 was a gift from Dr. Karl Johnson (Haverford University). Genetic crosses to determine allelism were performed using standard methods to produce stable diploids (Levine and Ebersold, 1960) and progeny were scored for motility and flagellar length phenotype using a Zeiss DR-C stereomicroscope (80X magnification) and a Zeiss Standard phase contrast microscope (400X magnification), respectively. For physical mapping, strain 3F12 was crossed to polymorphic strain S1 D2 (Gross *et al.*, 1988). Only one progeny from each tetrad was picked for PCR analysis so that each represented independent recombination events. Primers used for mapping (Table S1) were from Kathir *et al.* (2003), Rymarquis *et al.* (2005) or were developed in this project.

DNA and RNA analysis

Chlamydomonas DNA and Southern blot analysis were performed as described (Tam and Lefebvre, 1993). *Chlamydomonas* genomic libraries in bacteriophage lambda vectors were constructed using λ FixII/*Xho*I kit (Agilent Technologies) using *Mbo*I partially digested DNA from 21 gr or 3F12. For physical mapping of *LF5*, PCR was performed using Failsafe enzyme with premix K (Epicenter), on DNA prepared with DNeasy Plant Mini Kit (Qiagen). Primer sequences for mapping and PCR amplification of *LF5* are given in supplemental Table S1.

Total RNA and poly(A+) RNA were prepared as described (Nguyen *et al.*, 2005; Tam *et al.*, 2007). 25 μ g of total RNA or 5 μ g of poly(A+) RNA were size fractionated on 1% formaldehyde gels and transferred to Brightstar Plus membrane (Ambion), and hybridized successively with 32 P-labeled DNA from the entire *LF5* coding region (amplified from cDNA using 3830-5' and 3830-3' primers) or from *CRY1*. Radioactivity on membranes was quantified by exposing them to a phospho screen, which was scanned with a STORM 840 Imager and analyzed with ImageQuant v1.2 (Molecular Dynamics).

Cloning of *LF5*

A bacteriophage lambda library prepared with DNA from WT cells was screened with a *LF5* PCR probe amplified from a cDNA library using primers 3830-F1 and 3830-R2. The resulting clones were tested for their ability to rescue *lf5* mutants by co-transformation with pSII103 (Sizova *et al.* 2001). A 16-kb *Bam*HI-*Xba*I fragment from a lambda clone was subcloned into pBluescript II KS+ to produce plasmid pBS3830. To determine the insertion in 3F12, a lambda library of 3F12 was screened with the same probe. To verify the mRNA sequence, a *Chlamydomonas* cDNA library (G2, from *Chlamydomonas* Resource Center) was screened with a PCR probe made with 3830-F3 and R3. Six overlapping clones covering the entire coding region were recovered and sequenced.

Preparation of antibodies to LF5p

The entire coding region of *LF5* was amplified by PCR from a cDNA clone using 3830-5' and 3830-3' primers and *Pfu* Ultra DNA polymerase (Agilent Technologies), and cloned into pCR8/GW/TOPO (Invitrogen). After the sequence was verified, the cDNA was recombined using LR clonase (Invitrogen) into expression vectors pMCSG19C (Donnelly *et al.*, 2006) or pMAL, which have been made Gateway-cloning compatible by the insertion of the conversion cassette (generous gift from Dr. Neil Olszewski, University of Minnesota). Affinity-purified maltose-binding protein/LF5p or insoluble His-tagged LF5 fusion protein run and excised on acrylamide gel was used to immunize rabbits, UMN182 and UMN183, respectively. Both antibodies recognized the same protein bands on western blots but only UMN183 was used for subsequent studies because its titer was higher. For affinity purification, maltose-binding-protein/LF5 fusion protein was covalently linked to amylose resin in a column to purify UMN183. For western analysis, flagella were isolated as described in (Tam *et al.*, 2007). For fractionation studies, purified flagella was first extracted with 0.5% NP40 in HMEDNa (10 mM Hepes, pH 7.0, 5 mM MgSO₄, 0.5 mM EDTA, 1 mM DTT, 30 mM NaCl) supplemented with 1/100 volume of protease inhibitor cocktail (p-8340, Sigma-Aldrich), separated into soluble and insoluble fractions. The insoluble fraction was extracted either with 0.5 M NaCl or 0.6 M KI in HMEDNa, before separating into soluble and insoluble fractions. Equivalent amount of each fraction corresponding to 37.5 µg of flagella were electrophoresed on 8% acrylamide gels and transferred to PVDF membrane. Affinity purified UMN183 and goat anti-rabbit horseradish peroxidase conjugated secondary antibody (Sigma-Aldrich) were used at 1:250 and 1:22, 000, respectively. Amersham ECL Western Blotting Detection Reagents (GE Healthcare) were used as the chemiluminescent reagents.

Light microscopy and flagellar length measurements

Cells were fixed in 1% glutaraldehyde and visualized with DIC microscopy (Diaplan, Leica) with a 100X NA 1.25 objective (Leitz) using a digital camera (ProgRes® MFcool, Jenoptik) and ProgRes MAC CapturePro software. Images were opened with Image J (version 1.45s) and flagellar length was measured using the segmented line tool. For deflagellation experiments, cells were transferred to M medium and induced to shed their flagella by adding 0.005 volume of 1 M acetic acid to cells. As soon as deflagellation was complete, as verified by microscopy, 0.005 volume of 1 M potassium hydroxide was added to neutralize the medium. Cells were harvested by centrifugation and resuspended in fresh M medium to allow for flagellar regrowth. Regenerating cultures were sampled at different times and fixed for flagellar length measurement.

Immunofluorescence microscopy

For immunofluorescence, cells were treated with autolysin for 1 hour to remove cell walls, transferred to a solution of 10 mM Hepes, 5 mM MgSO₄, 0.5 mM EGTA, 25 mM KCl, and allowed to settle on polyethyleneimine-coated printed slides. The slides were dipped in methanol twice, for 10 min at -20 °C. Air-dried cell samples were blocked in blocking buffer (5% glycerol, 10% Normal Goat Serum, 1% BSA, 1% cold water fish gelatin, 5% DMSO in PBS) for 30 min, 37 °C. Primary antibodies were affinity-purified UMN183 at 1:100 dilution and 6-11-B1 (monoclonal acetylated α -tubulin; a gift from Dr. G. Piperno) at 1:50 dilution. Secondary antibodies were goat anti-rabbit Alexa Fluor 488 (Molecular Probes) and goat anti-mouse Texas Red (ICN-Cappel) or goat anti-mouse Alexa Fluor 568 (Molecular Probes), all at 1:400 dilution in blocking buffer. Samples were mounted in Slowfade (Invitrogen). DIC and fluorescent images were captured with the same microscope and software setup described above for light microscopy, assembled and adjusted with Photoshop CS5 (Adobe).

Dikaryon analysis

To make gametes, *lfl* (CC-1678) and WT (CC-125) cells were resuspended in 1-2 ml of autolysin made in minimal medium without nitrogen and incubated under lights for 4 hours. To start the mating reactions, 200 μ l samples of each gamete culture were mixed together in a microfuge tube. At the indicated times, the mating cultures were pelleted in a microcentrifuge, resuspended in 10 mM HEPES, 5 mM MgSO₄, 0.5 mM EGTA, 25 mM KCl, mounted on polyethyleneimine-coated coverslips, and processed for immunofluorescence as described above. Samples of the mating cultures and parent strains were fixed in glutaraldehyde for flagellar length measurement. For each parent cell and each dikaryon, the length of one flagellum of each pair of flagella was measured. If the two flagella of a cell were different in length as in some cases with *lfl*, the longer flagellum was measured.

Acknowledgements

We thank Drs. Karl Johnson, Neil Olszewski, Gianni Piperno and Mark Donnelly for provision of reagents used in this study. We are grateful to Dr. Lynn Hartweck for her advice with the Gateway cloning technology. We thank Matt Laudon and the Chlamydomonas Resource Center, University of Minnesota, for providing strains and mapping primers, and Dr. Carolyn Silflow for helpful suggestions on the manuscript. The work was supported by NIGMS grant GM34437 and NIDDK grant DK085392 to P.A.L.

References

- Asleson, C. M., and Lefebvre, P. A. (1998). Genetic analysis of flagellar length control in *Chlamydomonas reinhardtii*: a new long-flagella locus and extragenic suppressor mutations. *Genetics* 148, 693-702.
- Badano, J. L., Mitsuma, N., Beales, P. L., and Katsanis, N. (2006). The ciliopathies: an emerging class of human genetic disorders. *Annu. Rev. Genomics Hum. Genet.* 7, 125-148.
- Barsel, S. E., Wexler, D. E., and Lefebvre, P. A. (1988). Genetic analysis of long-flagella mutants of *Chlamydomonas reinhardtii*. *Genetics* 118, 637-648.
- Berbari, N. F., O'Connor, A. K., Haycraft, C. J., and Yoder, B. K. (2009). The primary cilium as a complex signaling center. *Curr. Biol.* 19, R526-535.

- Berman, S. A., Wilson, N. F., Haas, N. A., and Lefebvre, P. A. (2003). A novel MAP kinase regulates flagellar length in *Chlamydomonas*. *Curr. Biol.* *13*, 1145-1149.
- Bradley, B. A., and Quarmby, L. M. (2005). A NIMA-related kinase, Cnk2p, regulates both flagellar length and cell size in *Chlamydomonas*. *J. Cell Sci.* *118*, 3317-3326.
- Chen, Q., Zhu, Y. C., Yu, J., Miao, S., Zheng, J., Xu, L., Zhou, Y., Li, D., Zhang, C., Tao, J., and Xiong, Z. Q. (2010). CDKL5, a protein associated with Rett syndrome, regulates neuronal morphogenesis via Rac1 signaling. *J. Neurosci.* *30*, 12777-12786.
- Craige, B. C., Tsao, C., Diener, D. R., Hou, Y., Lechtreck, K. F., Rosenbaum, J. L., and Witman, G. B. (2010). CEP290 tethers flagellar transition zone microtubules to the membrane and regulates flagellar protein content. *J. Cell Biol.* *190*, 927-940.
- Diener, D. R., Ang, L. H., and Rosenbaum, J. L. (1993). Assembly of flagellar radial spoke proteins in *Chlamydomonas*: identification of the axoneme binding domain of radial spoke protein 3. *J. Cell Biol.* *123*, 183-190.
- Donnelly, M. I., Zhou, M., Millard, C. S., Clancy, S., Stols, L., Eschenfeldt, W. H., Collart, F. R., and Joachimiak, A. (2006). An expression vector tailored for large-scale, high-throughput purification of recombinant proteins. *Protein Expr. Purif.* *47*, 446-454.
- Dutcher, S. K., Huang, B., and Luck, D. J. (1984). Genetic dissection of the central pair microtubules of the flagella of *Chlamydomonas reinhardtii*. *J. Cell Biol.* *98*, 229-36.
- Dymek, E. E., and Smith, E. F. (2012). *PF19* encodes the catalytic subunit of katanin, p60, and is required for assembly of the flagellar central apparatus in *Chlamydomonas*. *J. Cell Sci.* *125*, 3357-3366.
- Engel, B. D., Ludington, W. B., and Marshall, W. F. (2009). Intraflagellar transport particle size scales inversely with flagellar length: revisiting the balance-point length control model. *J. Cell Biol.* *187*, 81-89.
- Gardner, L. C., O'Toole, E., Perrone, C. A., Giddings, T., and Porter, M. E. (1994). Components of a "dynein regulatory complex" are located at the junction between the radial spokes and the dynein arms in *Chlamydomonas* flagella. *J. Cell Biol.* *127*, 1311-1125.
- Grillo, E., Villard, L., Clarke, A., Ben Zeev, B., Pineda, M., Bahi-Buisson, N., Hryniewiecka-Jaworska, A., Bienvenu, T., Armstrong, J., Martinez, A. R., Mari, F., Veneselli, E., Russo, S., Vignoli, A., Pini, G., Djuric, M., Bisgaard, A. M., Mejaški Bošnjak, V., Polgár, N., Cogliati, F., Ravn, K., Pintaudi, M., Melegh, B., Craiu, D., Djukic, A., and Renieri, A. (2012). Rett networked database: an integrated clinical and genetic network of Rett syndrome databases. *Hum Mutat.* *33*, 1031-1036.
- Gross, C. H., Ranum, L. P. W., and Lefebvre, P. A. (1988). Extensive restriction fragment length polymorphisms in a new isolate of *Chlamydomonas reinhardtii*. *Curr. Genet.* *13*, 503-508.
- Hashimoto, M., Shinohara, K., Wang, J., Ikeuchi, S., Yoshida, S., Meno, C., Nonaka, S., Takada, S., Hatta, K., Wynshaw-Boris, A., and Hamada, H. (2010). Planar polarization of node

cells determines the rotational axis of node cilia. *Nat. Cell Biol.* *12*, 170-176.

Huang, B., Piperno, G., Ramanis, Z., and Luck, D. J. (1981). Radial spokes of *Chlamydomonas* flagella: genetic analysis of assembly and function. *J. Cell Biol.* *88*, 80-88.

Johnson, K. A., and Rosenbaum, J. L. (1992). Polarity of flagellar assembly in *Chlamydomonas*. *J. Cell Biol.* *119*, 1605-1611.

Kalscheuer, V. M., Tao, J., Donnelly, A., Hollway, G., Schwinger, E., Kübart, S., Menzel, C., Hoeltzenbein, M., Tommerup, N., Eyre, H., Harbord, M., Haan, E., Sutherland, G. R., Ropers, H. H., and Gécz, J. (2003). Disruption of the serine/threonine kinase 9 gene causes severe X-linked infantile spasms and mental retardation. *Am. J. Hum. Genet.* *72*, 1401-1411.

Kameshita, I., Sekiguchi, M., Hamasaki, D., Sugiyama, Y., Hatano, N., Suetake, I., Tajima, S., and Sueyoshi, N. (2008). Cyclin-dependent kinase-like 5 binds and phosphorylates DNA methyltransferase 1. *Biochem. Biophys. Res. Commun.* *377*, 1162-1167.

Kamiya, R. (1988). Mutations at twelve independent loci result in absence of outer dynein arms in *Chlamydomonas reinhardtii*. *J. Cell Biol.* *107*, 2253-2258.

Kathir, P., LaVoie, M., Brazelton, W. J., Haas, N. A., Lefebvre, P. A., and Silflow, C. D. (2003). Molecular map of the *Chlamydomonas reinhardtii* nuclear genome. *Euk. Cell* *2*, 362-379.

Kato-Minoura, T., Hirono, M., and Kamiya, R. (1997). *Chlamydomonas* inner-arm dynein mutant, *ida5*, has a mutation in an actin-encoding gene. *J. Cell Biol.* *137*, 649-656.

Kilstrup-Nielsen, C., Rusconi, L., La Montanara, P., Ciceri, D., Bergo, A., Bedogni, F., and Landsberger, N. (2012). What we know and would like to know about CDKL5 and its involvement in epileptic encephalopathy. *Neural Plast.* *2012*, 728267.

King, S. J., and Dutcher, S. K. (1997). Phosphoregulation of an inner dynein arm complex in *Chlamydomonas reinhardtii* is altered in phototactic mutant strains. *J. Cell Biol.* *136*, 177-191.

King, S. M. (2006). Axonemal protofilament ribbons, DM10 domains, and the link to juvenile myoclonic epilepsy. *Cell Motil. Cytoskeleton* *63*, 245-253.

Kuchka, M.R., and Jarvik J.W. (1987). Short-Flagella Mutants of *Chlamydomonas reinhardtii*. *Genetics* *115*, 685-691.

Lefebvre, P. A., Nordstrom, S. A., Moulder, J. E., and Rosenbaum, J. L. (1978). Flagellar elongation and shortening in *Chlamydomonas*. IV. Effects of flagellar detachment, regeneration, and resorption on the induction of flagellar protein synthesis. *J. Cell Biol.* *78*, 8-27.

Levine, R. P., and Ebersold, W. T. (1960). The genetics and cytology of *Chlamydomonas*. *Annu. Rev. Microbiol.* *14*, 197-216.

Luck, D., Piperno, G., Ramanis, Z., and Huang, B. (1977). Flagellar mutants of *Chlamydomonas*: studies of radial spoke-defective strains by dikaryon and revertant analysis. *Proc. Natl. Acad. Sci. U. S. A.* *74*, 3456-3460.

- Luo, M., Cao, M., Kan, Y., Li, G., and Pan, J. (2011). The phosphorylation state of an aurora-like kinase marks the length of growing flagella in *Chlamydomonas*. *Curr. Biol.* *21*, 586-591.
- Mahjoub, M. R., Rasi, M. Q., and Quarmby, L. M. (2004). Fa2p, localizes to a novel site in the proximal cilia of *Chlamydomonas* and mouse kidney cells. *Mol. Biol. Cell* *15*, 5172-5186.
- Mastrorade, D. N., O'Toole, E.T., McDonald, K. L., McIntosh, J. R., and Porter, M. E.. (1992). Arrangement of inner dynein arms in wild-type and mutant flagella of *Chlamydomonas*. *J. Cell Biol.* *118*, 1145-1162.
- Myster, S. H., Knott, J. A., O'Toole, E., and Porter, M. E. (1997). The *Chlamydomonas* Dhc1 gene encodes a dynein heavy chain subunit required for assembly of the II inner arm complex. *Mol. Biol. Cell* *8*, 607-20.
- Nelson, J. S., Savereide, P. B., and Lefebvre, P. A. (1994). The CRY1 gene in *Chlamydomonas reinhardtii*: structure and use as a dominant selectable marker for nuclear transformation. *Mol. Cell. Biol* *6*, 4011-4019.
- Nguyen, R. L., Tam, L.-W., and Lefebvre, P. A. (2005). The *LF1* gene of *Chlamydomonas reinhardtii* encodes a novel protein required for flagellar length control. *Genetics* *169*, 1415-1424.
- Ou, Y., Ruan, Y., Cheng, M., Moser, J. J., Rattner, J. B., and van der Hoorn, F. A. (2009). Adenylate cyclase regulates elongation of mammalian primary cilia. *Exp. Cell Res.* *315*, 2802-2817.
- Pazour, G. J., Wilkerson, C. G., and Witman, G. B. (1998). A dynein light chain is essential for the retrograde particle movement of intraflagellar transport (IFT). *J. Cell Biol.* *141*, 979-992.
- Pazour, G. J., Agrin, N., Leszyk, J., and Witman, G. B. (2005). Proteomic analysis of a eukaryotic cilium. *J. Cell Biol.* *170*, 103-113.
- Pedersen, L. B., Miller, M. S., Geimer, S., Leitch, J. M., Rosenbaum, J. L., and Cole, D.G. (2005). *Chlamydomonas* IFT172 is encoded by *FLA11*, interacts with CrEB1, and regulates IFT at the flagellar tip. *Curr. Biol.* *15*, 262-266.
- Piperno, G., Ramanis, Z., Smith, E. F., and Sale, W. S. (1990). Three distinct inner dynein arms in *Chlamydomonas* flagella: molecular composition and location in the axoneme. *J. Cell Biol.* *110*, 379-389.
- Piperno, G., Mead, K., and Shestak, W. (1992). The inner dynein arms I2 interact with a "dynein regulatory complex" in *Chlamydomonas* flagella. *J. Cell Biol.* *118*, 1455-1463.
- Qin, H., Diener, D. R., Geimer, S., Cole, D. G., and Rosenbaum, J. L. (2004). Intraflagellar transport (IFT) cargo: IFT transports flagellar precursors to the tip and turnover products to the cell body. *J. Cell Biol.* *164*, 255-266.
- Rademacher, N., Hambrock, M., Fischer, U., Moser, B., Ceulemans, B., Lieb, W., Boor, R., Stefanova, I., Gillessen-Kaesbach, G., Runge, C., Korenke, G.C., Spranger, S., Laccone, F., Tzschach, A., and Kalscheuer, V. M. (2011). Identification of a novel CDKL5 exon and pathogenic mutations in patients with severe mental retardation, early-onset seizures and Rett-

like features. *Neurogenetics* 12, 165-167.

Ricciardi, S., Kilstrup-Nielsen, C., Bienvenu, T., Jacquette, A., Landsberger, N., and Broccoli, V. (2009). CDKL5 influences RNA splicing activity by its association to the nuclear speckle molecular machinery. *Hum. Mol. Genet.* 18, 4590-4602.

Rusconi, L., Salvatoni, L., Giudici, L., Bertani, I., Kilstrup-Nielsen, C., Broccoli, V., and Landsberger, N. (2008). CDKL5 expression is modulated during neuronal development and its subcellular distribution is tightly regulated by the C-terminal tail. *J. Biol. Chem.* 283, 30101-30111.

Rymarquis, L. A., Handley, J. M., Thomas, M., and Stern, D. B. (2005). Beyond complementation. Map-based cloning in *Chlamydomonas reinhardtii*. *Plant Physiol.* 137, 557-566.

Sanders, M. A., and Salisbury, J. L. (1989). Centrin-mediated microtubule severing during flagellar excision in *Chlamydomonas reinhardtii*. *J. Cell Biol.* 108, 1751-1760.

Scholey, J. M. (2003). Intraflagellar transport. *Annu. Rev. Cell Dev. Biol.* 19, 423-443.

Segal, R. A., Huang, B., Ramanis, Z., and Luck, D. J. (1984). Mutant strains of *Chlamydomonas reinhardtii* that move backwards only. *J. Cell Biol.* 98, 2026-2034.

Sizova, I., Fuhrmann, M., and Hegemann, P. (2001). A *Streptomyces rimosus* APHVIII gene coding for a new type phosphotransferase provides stable antibiotic resistance to *Chlamydomonas reinhardtii*. *Gene* 277, 221-229.

Smith, E. F., and Lefebvre, P. A. (1996). *PF16* encodes a protein with armadillo repeats and localizes to a single microtubule of the central apparatus in *Chlamydomonas* flagella. *J. Cell Biol.* 132, 359-370.

Smith, E. F., and Lefebvre, P. A. (1997). *PF20* gene product contains WD repeats and localizes to the intermicrotubule bridges in *Chlamydomonas* flagella. *Mol. Biol. Cell* 8, 455-467.

Stolc, V., Samanta, M. P., Tongprasit, W., and Marshall, W. F. (2005). Genome-wide transcriptional analysis of flagellar regeneration in *Chlamydomonas reinhardtii* identifies orthologs of ciliary disease genes. *Proc. Natl. Acad. Sci. USA*, 32:3703-3707.

Tam, L.-W., and Lefebvre, P. A. (1993). Cloning of flagellar genes in *Chlamydomonas reinhardtii* by DNA insertional mutagenesis. *Genetics* 135, 375-384.

Tam, L.-W., Dentler, W. L., and Lefebvre, P. A. (2003). Defective flagellar assembly and length regulation in *LF3* null mutants in *Chlamydomonas*. *J. Cell Biol.* 163, 597-607.

Tam, L.-W., Wilson, N. F., and Lefebvre, P. A. (2007). A CDK-related Kinase Regulates the Length and Assembly of Flagella in *Chlamydomonas*. *J. Cell Biol.* 176, 819-829.

Wemmer, K. A., and Marshall, W. F. (2007). Flagellar length control in *Chlamydomonas*--paradigm for organelle size regulation. *Int. Rev. Cytol.* 260, 175-212.

Williamson, S. L., Giudici, L., Kilstrup-Nielsen, C., Gold, W., Pelka, G. J., Tam, P. P., Grimm, A., Prodi, D., Landsberger, N., and Christodoulou, J. (2012). A novel transcript of cyclin-dependent kinase-like 5 (CDKL5) has an alternative C-terminus and is the predominant transcript in brain. *Hum. Genet.* 131, 187-200.

Wilson, N. F., and Lefebvre, P. A. (2004). Regulation of flagellar assembly by glycogen synthase kinase 3 in *Chlamydomonas reinhardtii*. *Eukaryot. Cell* 3, 1307-1319.

Wilson, N. F., Iyer, J. K., Buchheim, J. A., and Meek, W. (2008). Regulation of Flagellar Length in *Chlamydomonas*. *Semin. Cell Dev. Biol.* 19, 494-501.

Witman, G. B. (1975). The site of *in vivo* assembly of flagellar microtubules. *Ann. N. Y. Acad.*

Sci. 253, 178-191.

Witman, G. B., Plummer, J., and Sander, G. (1978). Chlamydomonas flagellar mutants lacking radial spokes and central tubules. Structure, composition, and function of specific axonemal components. *J. Cell Biol.* 76:729-747.

Yagi, T., Uematsu, K., Liu, Z., and Kamiya, R. (2009). Identification of dyneins that localize exclusively to the proximal portion of Chlamydomonas flagella. *J. Cell Sci.* 122, 1306-1314.

Table 1. Mapping distance of molecular markers on chromosome 12 to 3F12 mutation

<u>Markers</u>	<u>Location (bp) ^a</u>	<u>Mapped distance in cM^b</u>
RDG	7400000	14.7 (34)
TUB2	7700000	15.6 (45)
8820	8820000	6.8 (47)
14-3-3	9000000	4.3 (46)
9280	9280000	0 (79)
6330	6330000	0 (96)
6170	6170000	0 (124)
ODA9	6070000	0 (43)
6000	6000000	0 (123)
5750	5750000	3.3 (92)

^aApproximate position of markers is given according to JGI Chlre4 (<http://genome.jgi-psf.org/Chlre4/Chlre4.info.html>). The centromere is located between marker 9280 and 6330, and has apparently disrupted the linearity of sequence assembly within this region in the JGI genomic database.

^bThe number of progeny used for mapping is given in parentheses.

Table 2. Percentage of cells with different localization pattern of LF5p

	Proximal only	Distal only	Proximal and distal	Along flagella only
WT	100/98.1	0/0	0/1.9	0/0
<i>lf1-1</i>	1.8/0	65.5/77.8	32.7/20.4	0/1.9
<i>lf2-1</i>	3.4/0	44.3/56.3	49.2/40.0	3.5/3.6
<i>lf2-5</i>	10.4/6.8	37.9/44.4	46.5/42.6	5.2/5.6
<i>lf3-2</i>	0/0	90.2/88.0	7.8/2.0	2.0/10.0
<i>lf4-9</i>	96.4/83.6	0/0	3.6/16.4	0/0

Numbers denote percentage of flagella with one of the four localization patterns from two different experiments. Punctate staining may also be present with the first three localization patterns. 50-61 flagella were scored.

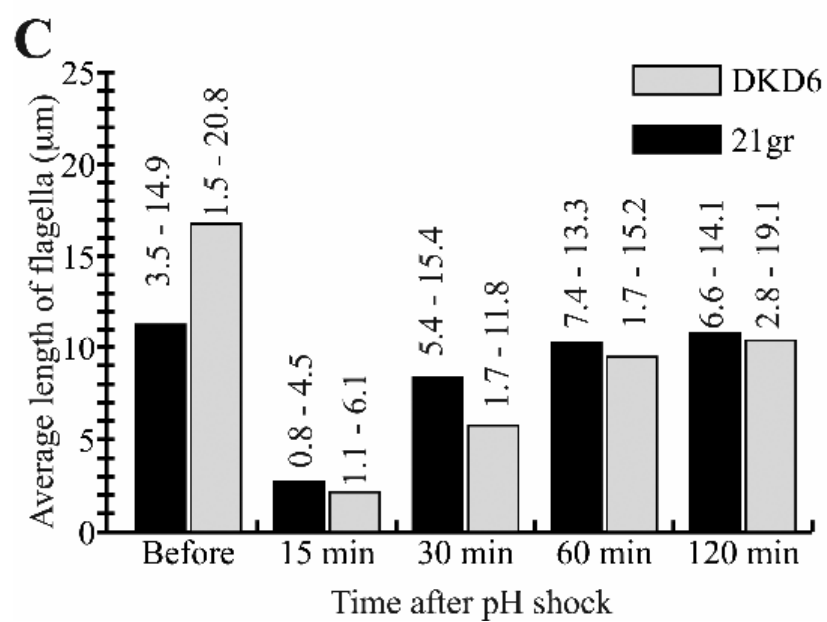
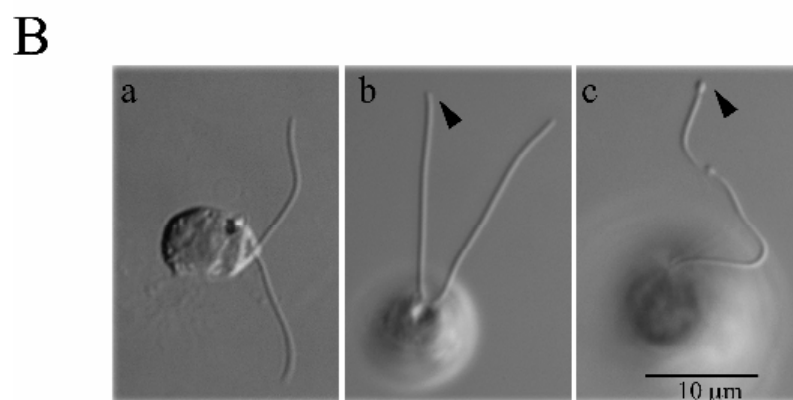
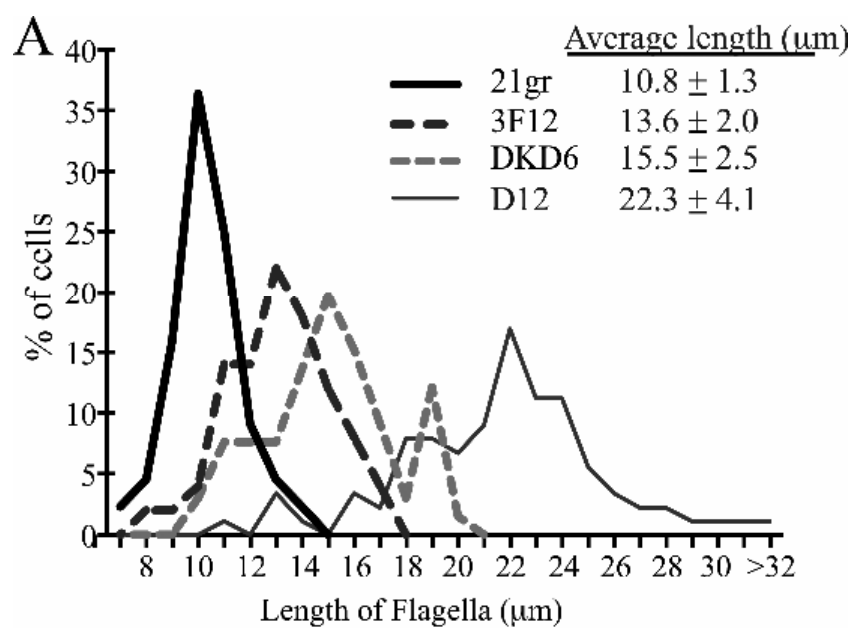


Figure 1. Long-flagella phenotype of new LF mutants. (A) Flagellar length distribution in vegetative populations of 21gr (WT), 3F12, DKD6, and D12 (*lf4-9*). The average flagellar lengths and standard deviations are shown. 50-89 cells were used for each measurement. (B) DIC images of (a) WT cells, (b) 3F12 and (c) *lf1-1* mutant. Arrowheads point to the tapered distal ends of 3F12 flagella and the swollen ends of *lf1-1* flagella. (C) The histogram shows the average flagellar length of flagellated cells before and at different times after pH-induced deflagellation. The percentage of cells with no flagella is highest at 15 min: 13.8% and 8.1% for 21gr and DKD6, respectively, and is less than 5% at all other time points. The range of flagellar length for each sample is shown on top of each histogram. 52-60 cells were measured.

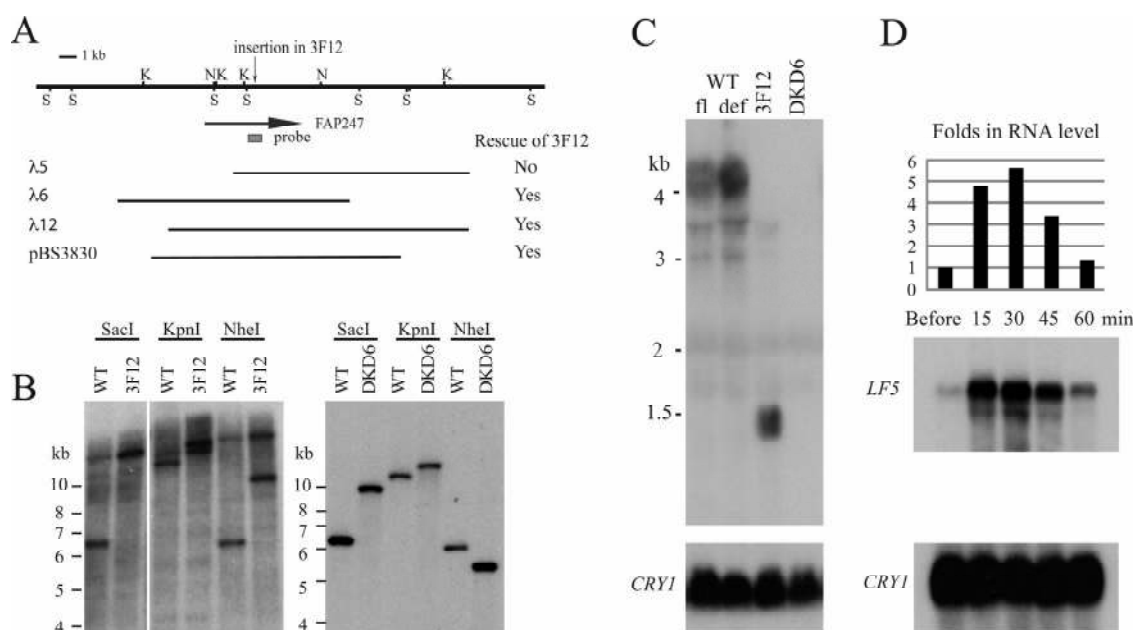


Figure 2. Genomic DNA and RNA analysis of *lf5* mutants. (A) Restriction map of the genomic region around a flagellar protein gene model, FAP247. Restriction sites are *SacI* (S), *KpnI* (K) and *NheI* (N). The gray box indicates the position of the genomic region used as a hybridization probe for Southern blots. (B) Disruption of FAP247 was detected in both 3F12 and DKD6 by Southern analysis using a PCR probe from the last exon of the gene model as indicated in (A). (C) Total RNA from WT cells before (“fl”) and 45 min (“def”) after deflagellation by pH shock, as well as 3F12 (*lf5-1*) and DKD6 (*lf5-2*), was size-fractionated on formaldehyde gels and hybridized successively to a cDNA probe covering the entire coding region of *LF5* (upper panel) and *CRY1* as a loading control (lower panel; Nelson *et al.*, 1994). A 4-kb transcript was detected in WT cells but not in the two *lf5* mutants. In *lf5-1*, a smaller transcript of approximately 1.5 kb was detected. (D) Poly(A)+ RNA samples from different times after WT cells were deflagellated by pH shock and allowed to regrow their flagella were analyzed. The level of *LF5* transcript was quantified and normalized to the level of *CRY1* transcript (lower panel) and shown as ratios to the normalized level before deflagellation. Levels of the *LF5* transcript increased rapidly within minutes after deflagellation.

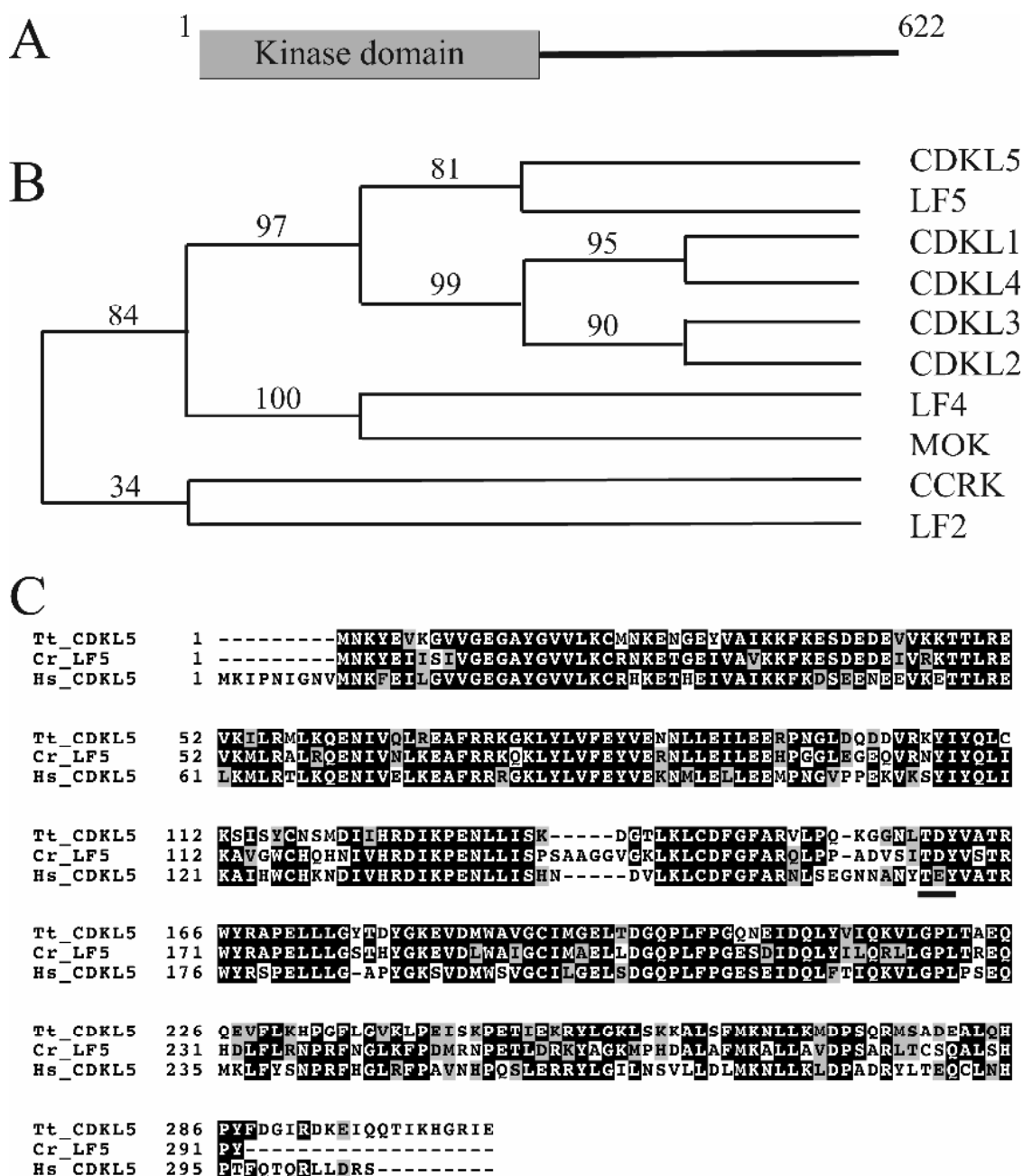


Figure 3. LF5p is a serine-protein kinase most closely related to CDKL5. (A) Schematic representation of the primary structure of LF5p, which has a N-terminal kinase domain and a novel C-terminal tail. (B) A cladogram of *Chlamydomonas* LF2, LF4 and LF5 showing the relationship to their closest human orthologs, constructed using Phylogeny.fr (www.phylogeny.fr). The numbers indicate branch support values in %. The GenBank accession numbers of the sequences are: NP_004187 (CDKL1), NP_003939 (CDKL2), NP_001107047 (CDKL3), NEAX00349 (CDKL4), NP_003150 (CDKL5), NP_055041 (MOK), NP_001034892 (CCRK), ABK34487 (LF2) and AAO86688 (LF4). (C) Alignment of the kinase domain of LF5p (Cr_LF5) to human (Hs_CDKL5) and Tetrahymena (Tt_CDKL5; XP_001008848) CDKL5. TE(D)Y motif is underlined.

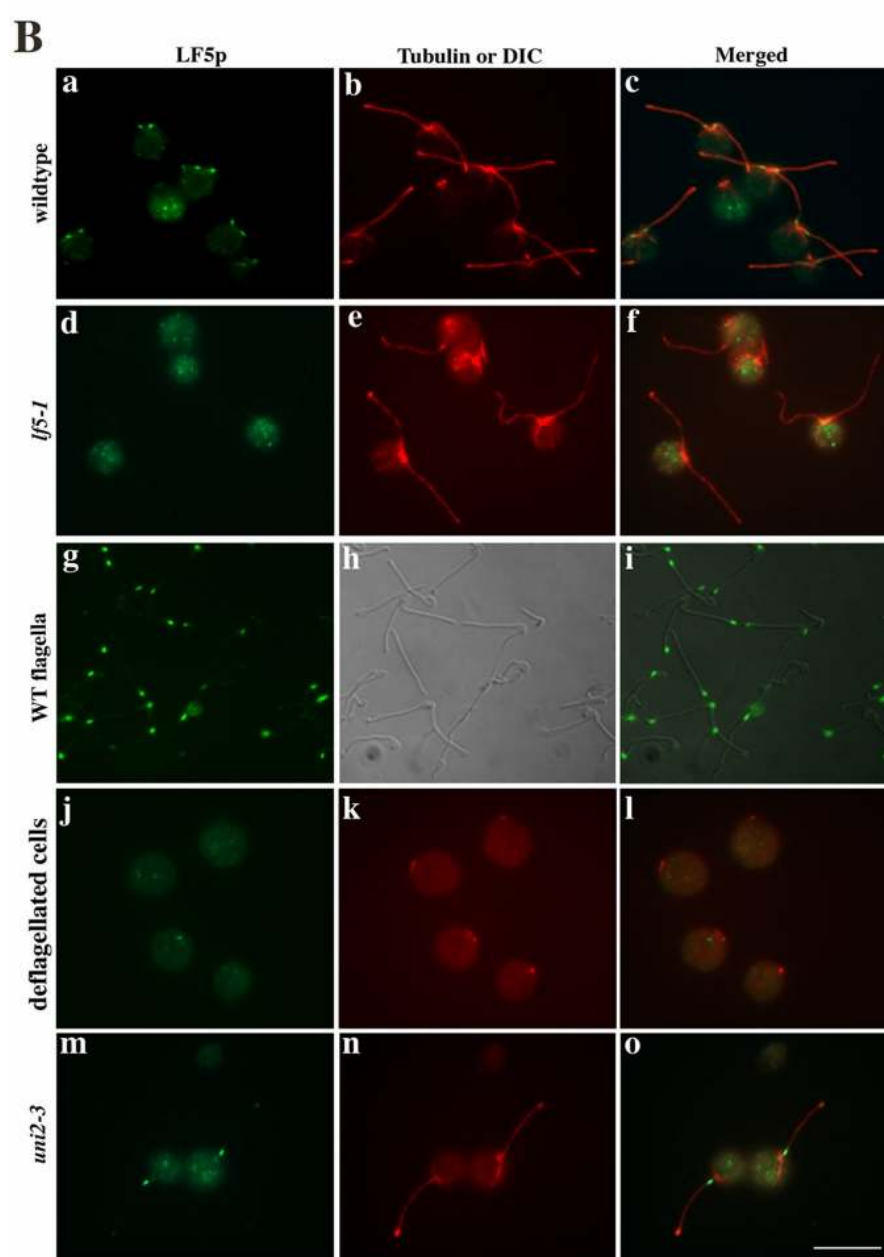
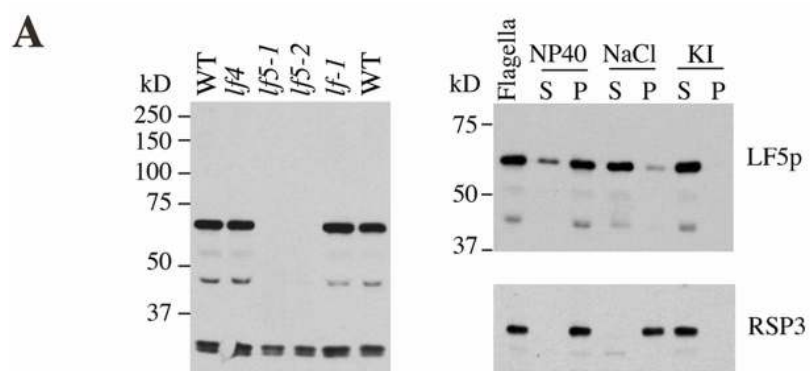


Figure 4. Western analysis and immunofluorescent localization of LF5p. (A) Western blot analysis of 37.5 μ g of purified flagella identified a major protein band of 66 kDa and a minor band of 45 kDa in WT, *lf1* and *lf4* cells (left panel). In the right panel, flagella were first extracted with 0.5% NP-40 and separated into soluble (S) and insoluble (P) fractions. The insoluble fraction was subsequently extracted with either 0.5 M NaCl or 0.6 M KI. The majority of the 66-kDa LF5p band was found in the NP-40 insoluble fraction, and could be solubilized with 0.5 M NaCl or 0.6 M KI. A control antibody against RSP3 shows the solubility of that radial spoke component. (B) Indirect immunofluorescence microscopy of (a-c) WT cells, (d-f) *lf5-1*, (g-i) detached flagella, (j-l) deflagellated cells obtained by pH shock and (m-o) *uni2-3* mutant cells with a single flagellum, using an antibody to LF5p (green) and an antibody to acetylated α -tubulin (red). LF5p localized specifically to the proximal ends of WT flagella. The conspicuous tubulin staining on the distal ends of some of the flagella were caused by curling up of the distal ends of flagella, an occasional artifact produced during methanol fixation. In panel g-i, the bright LF5p staining was only found on the non-swollen proximal ends of detached flagella. Bar, 10 μ m.

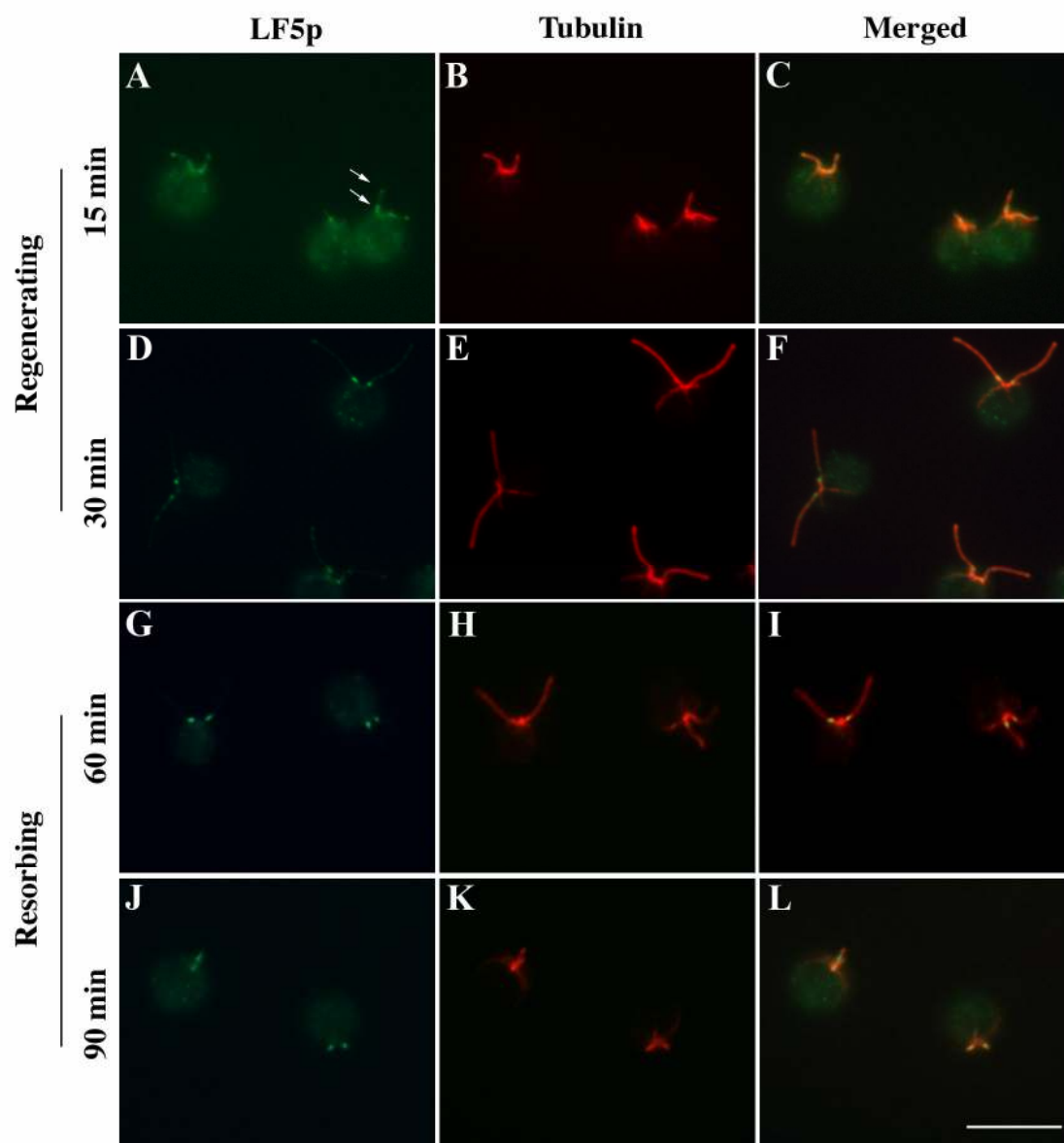


Figure 5. Immunofluorescence localization of LF5p during flagellar regeneration and resorption in WT cells. Green: LF5p, Red: acetylated α -tubulin. (A-C) Cells regrowing flagella 15 min after deflagellation showed LF5p staining at the proximal region as well as spotty staining along the entire length of the flagella. Arrows point to the staining on one flagellum. (D-F) At 30 min after pH shock, LF5p became more concentrated at the proximal region of flagella and less staining was observed along the length of the flagella. (G-L) Cells undergoing flagellar resorption induced by the addition of 20 mM sodium pyrophosphate. At 60 min after treatment with pyrophosphate, flagella were about half length. At 90 min, many flagella were resorbed to short stubs. Prominent LF5p staining was observed at the proximal region of flagella at all stages of resorption. Bar, 10 μ m.

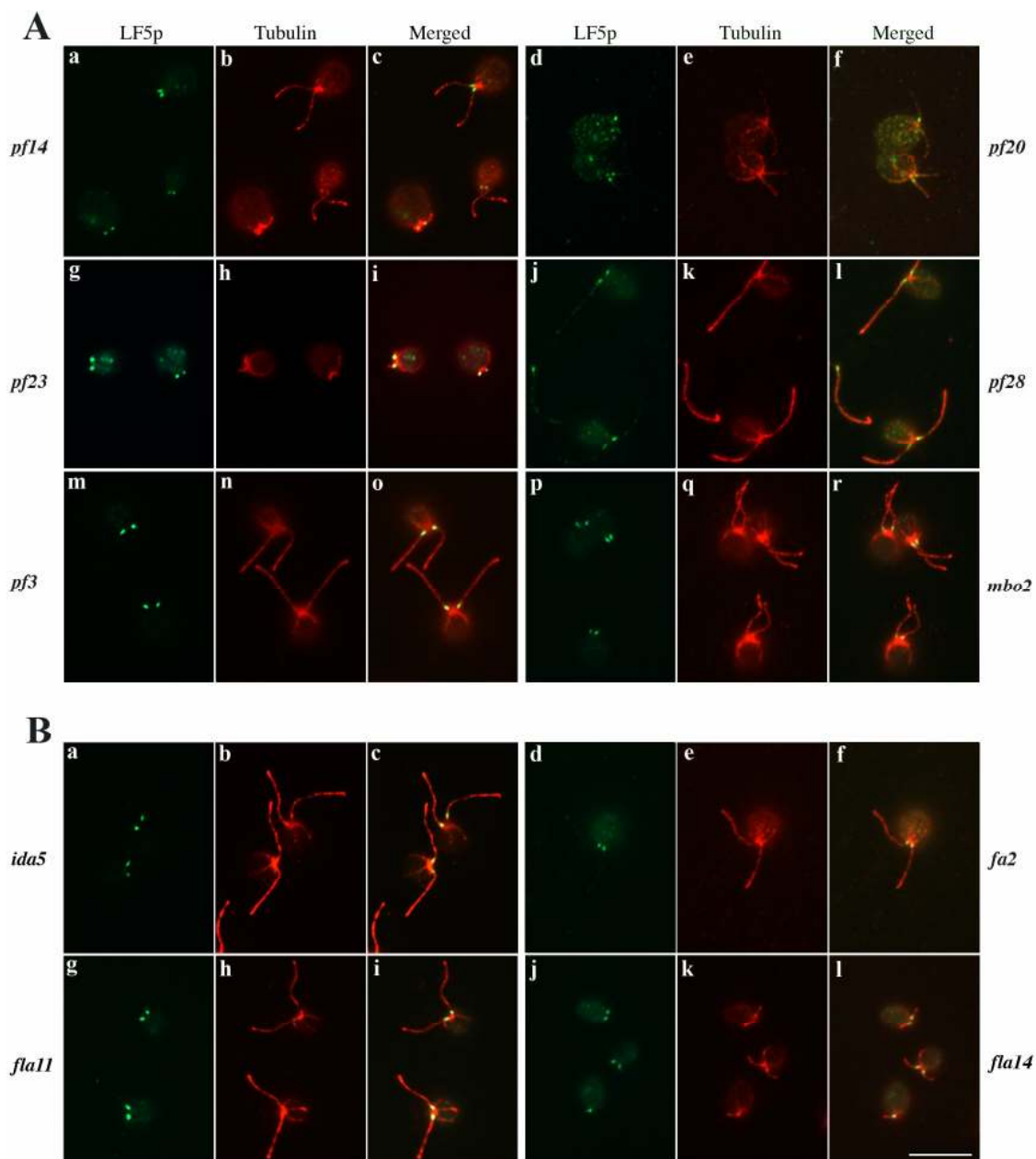


Figure 6. Immunofluorescence microscopy shows proximal localization of LF5p in various flagellar mutants. Green: LF5p, red: acetylated α -tubulin. (A) LF5p localization in various axonemal mutants defective in (a-c) radial spokes (*pf14*), (d-f) central pair microtubules (*pf20*), (g-i) inner-arm dyneins (*pf23*), (j-l) outer-arm dyneins (*pf28*), (m-o) dynein regulatory complex (*pf3*) and (p-r) beak projections (*mbo2*). (B) LF5p was localized to the proximal ends of flagella in (a-c) *ida5* and (d-f) *fa2* mutants, whose flagella lack DHC11 and FA2 proteins, respectively. Both DHC11 and FA2 have shown to be localized to proximal ends of flagella, but their absence did not affect the localization of LF5p. LF5p localization also appeared normal in IFT mutants, (g-i) *fla11* and (j-l) *fla14*, which have been shown to over-accumulate IFT proteins in their flagella. Bar, 10 μ m.

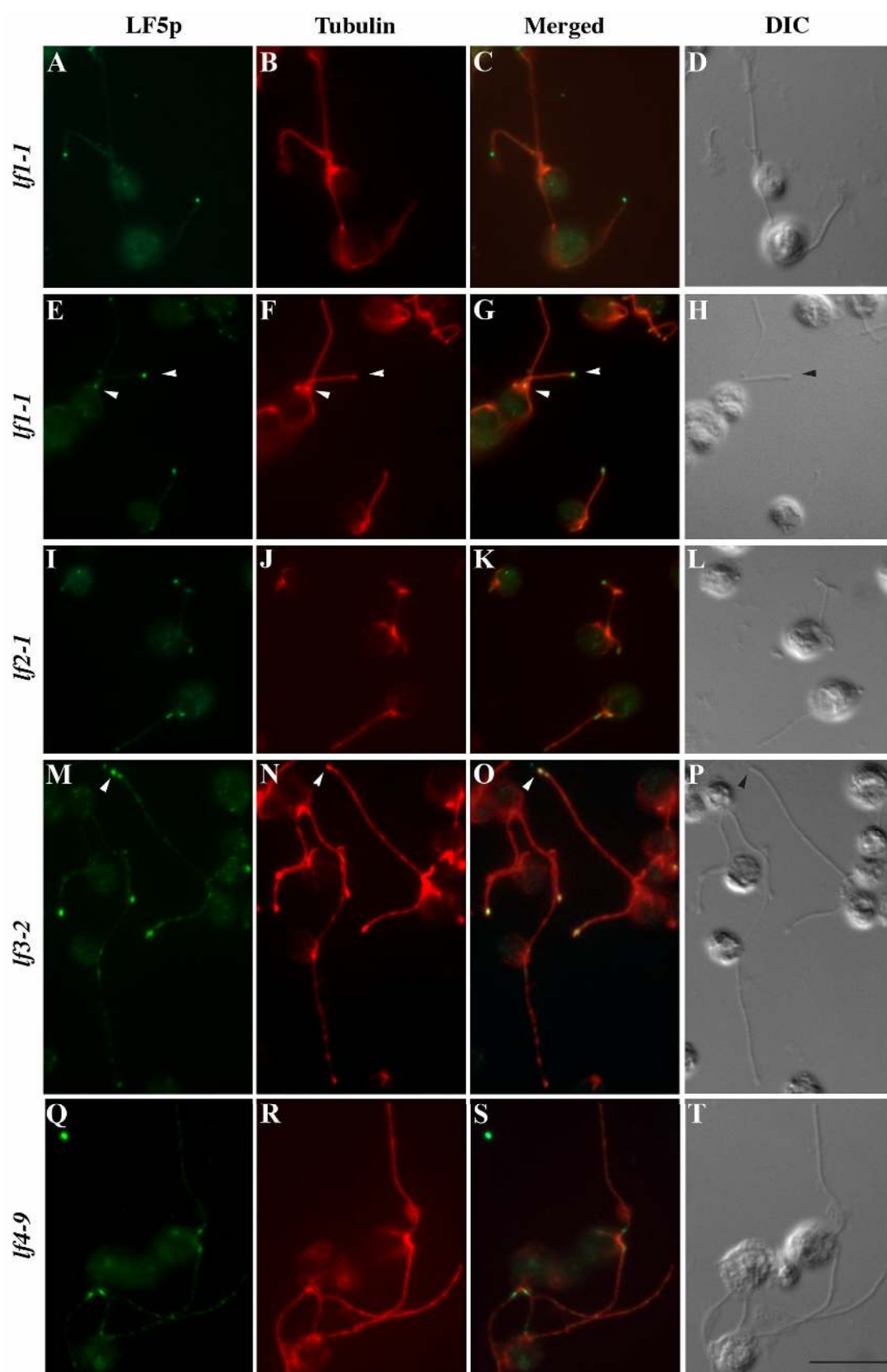


Figure 7. Immunofluorescence microscopy shows altered LF5p localization in *lf1*, *lf2* and *lf3* mutants. Green: LF5p, red: acetylated α -tubulin, DIC = differential interference contrast. (A-H) LF5p staining was often present at the distal tips of flagella in *lf1-1* mutants. Sometimes both distal and proximal LF5p staining could be seen on the same flagellum. Arrowheads in panels E-G point to the dual fluorescent spots of LF5p on a single flagellum. (I-L) *lf2-1* is a severe allele that is not expected to produce any functional LF2p and often has a pair of flagella that greatly differ in length. LF5p staining was present on the distal tips of the two unequal-length flagella on one cell, but on the proximal ends of another pair of flagella on another cell. In both *lf1-1* and *lf2-1* mutant flagella, the distal ends are often swollen, as indicated by the arrowhead in panel H. (M-P) In the *lf3-2* mutant, LF5p also localized abnormally to the distal ends of flagella (arrowheads). Punctate staining of LF5p could be seen on these flagella. (Q-T) LF5p localization remained predominantly proximal in *lf4-9* mutants. More punctate staining was observed along the length of flagella in *lf4-9* cells compared to WT cells (see Figure 4B). Bar, 10 μ m.

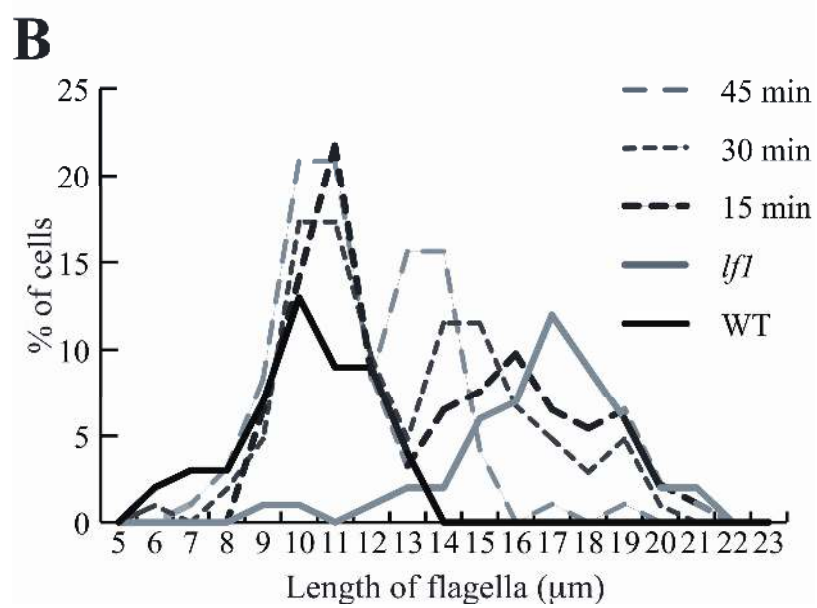
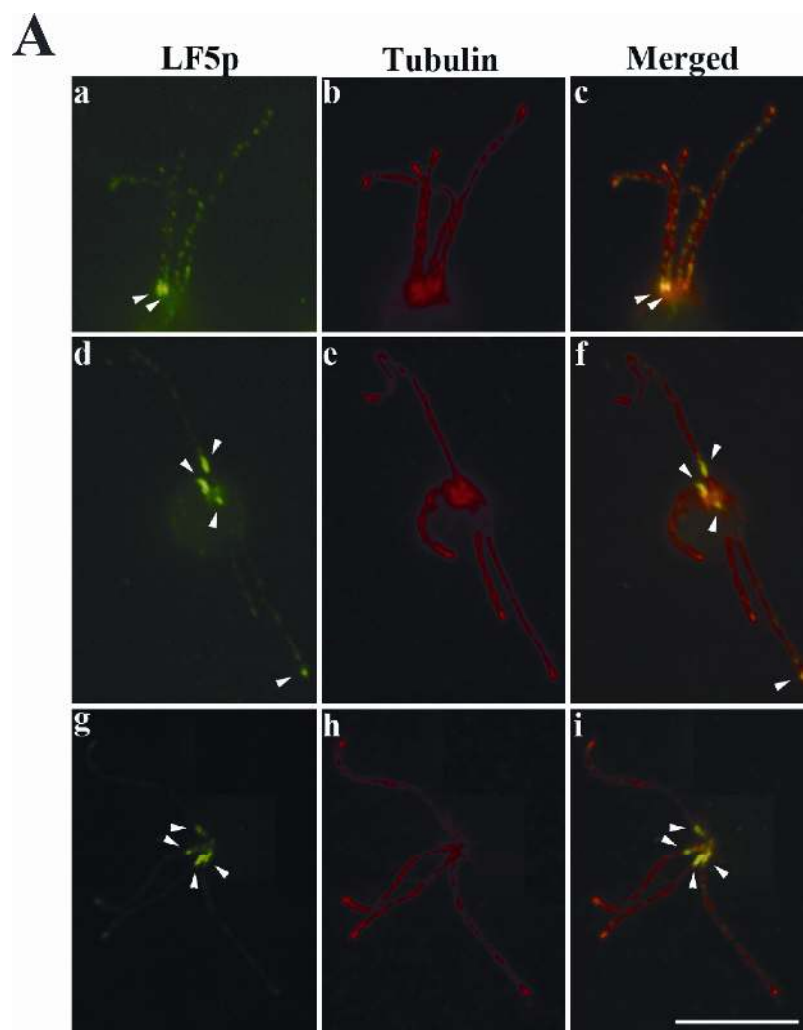


Figure 8. Relocalization of LF5p to the basal region of *lfl* flagella in dikaryons precedes rescue of flagellar length. (A) Immunofluorescence images showing different patterns of LF5p staining in dikaryons with a pair of shorter and a pair of longer flagella during a cross of *lfl* to WT gametes. Green:LF5p, red: α -tubulin. Arrowheads point to the position of LF5p determined by immunofluorescence. (a-c) no relocalization: with only two proximal stained spots on the shorter pair of flagella from the WT parent; (d-f) incomplete relocalization: proximal staining on the shorter pair of flagella and one of the pair of long flagella, with distal staining on the other long flagellum; (g-i) complete relocalization: four proximal stained spots on all four flagella. One pair of flagella is longer than the other pair. Bar, 10 μ m. (B) Flagellar length distribution of the parental WT and *lfl* cells, and dikaryons at different times after mating. Since two measurements were made for each dikaryon and only one per a single cell, the data for the WT and *lfl* cells were halved so that the height of the graphs are comparable. In dikaryons, the flagella from WT and *lfl* cells are clearly distinguishable, as indicated by the bimodal distribution pattern. At 15 min after mating, the longer flagella in dikaryons are similar in length as the *lfl* parent. The mutant pair of flagella gradually shortened in dikaryons over time but they had not completely resorbed to WT length even at 45 min.